Astron. Astrophys. 326, 682–691 (1997)

ASTRONOMY
AND
ASTROPHYSICS

The X-ray luminosity of rotation-powered neutron stars

W. Becker and J. Trümper

Max-Planck-Institut für Extraterrestrische Physik, D-85740 Garching bei München, Germany

Received 2 January 1997 / Accepted 30 April 1997

Abstract. As a result of recent observations with ROSAT and ASCA the number of rotation-powered pulsars seen at X-ray energies has increased substantially. In this paper we review the phenomenology of the observed X-ray emission properties. At present 27 pulsars are detected, representing a wide range of ages ($10^3 - 7 \times 10^9$ yrs), magnetic field strength ($10^8 - 10^{13}$ G) and spin periods ($1.6 - 530$ ms). Despite these dispersions in parameters all pulsars show an X-ray luminosity closely correlated with the rotational energy loss. This suggests that most of the observed X-rays are produced by magnetospheric emission originating from the co-rotating magnetosphere. Only for three middle aged pulsars (PSR 0656+14, Geminga and PSR 1055-52) and probably for the Vela-pulsar an additional thermal component is detected which can be attributed to thermal emission from the neutron stellar surface.

Key words: pulsars: general – X-rays: stars – stars: neutron

1. Introduction

The nearly 750 radio pulsars detected so far are interpreted as rapidly spinning and strongly magnetized neutron stars which are radiating at the expense of rotational energy (Pacini 1967). Although the popular model of magnetic braking provides plausible estimates for the neutron star magnetic dipole component $B_\perp$, its braking energy $\dot{E}$ and characteristic age τ, it does not provide any detailed information about the physical mechanism which operates in the pulsar magnetosphere and which is responsible for the broad band spectrum from the radio to the X- and gamma-ray bands. As a consequence, there exist a number of magnetospheric emission models, but no accepted theory. A recent review of the observational and theoretical situation is given in the proceedings of the IAU Colloquium 160 (Johnston, Walker & Bailes 1996).

In this paper we review the observed emission properties of rotation-powered neutron stars in the soft X-ray band. This radiation has been attributed to various thermal and non-thermal emission processes including

- Non-thermal emission from relativistic particles accelerated in the pulsar magnetosphere. The emission is characterized by a power-law spectrum (cf. Michel 1991 and references therein).
- Photospheric emission from the hot surface of a cooling neutron star. In this case a modified black-body spectrum and smooth, low amplitude variations with rotational phase are expected (cf. Greenstein & Hartke 1983; Romani 1987; Pavlov et al. 1995).
- Thermal emission from the neutron star's polar caps which are heated by the bombardment of relativistic particles streaming back to the surface from the pulsar magnetosphere (Kundt & Schaaf 1993; Zavlin, Shibanov & Pavlov 1995; Gil & Krawczyk 1996).
- Extended emission from a pulsar driven synchrotron nebula (cf. Michel 1991 and references therein).
- Soft X-ray emission from a relativistic pulsar wind or from a possible interaction of that wind with the interstellar medium or with a close companion star (bow shock nebula) (cf. Arons & Tavani 1993).

For a long time the most luminous of all rotation-powered pulsars, the Crab pulsar, had been the only radio pulsar detected at X-ray energies. With increasing sensitivity of the optical, X- and gamma-ray observations the number of pulsars detected in these spectral bands has steadily increased. At present 8 optical, 27 X-ray and 6 gamma-ray detections are known (cf. Table 3 and Fig.1). In X-rays, the first big step was taken with the Einstein Observatory which led to the discovery of pulsations from the Crab-like pulsars PSR 0540-69 and PSR 1509-58, while fluxes were found for PSR 0656+14, PSR 1055-52, PSR 1929+10 and PSR 0950+08 (cf. Seward & Wang 1988). More recently, ROSAT ($0.1 - 2.4$ keV) and ASCA ($\sim 0.7 - 10$ keV) have provided 18 and 2 further detections, respectively, including 8 pulsars for which X-ray pulsations were discovered. In addition, the superior sensitivity and spectral resolution of the ROSAT **P**osition **S**ensitive **P**roportional **C**ounter (PSPC) provided more detailed spectral information for a number of pulsars especially in the soft band ($0.1 - 0.6$ keV). Using the good angular resolution of the ROSAT **H**igh **R**esolution **I**mager nebular components could be identified and subtracted.

Send offprint requests to: web@mpe-garching.mpg.de

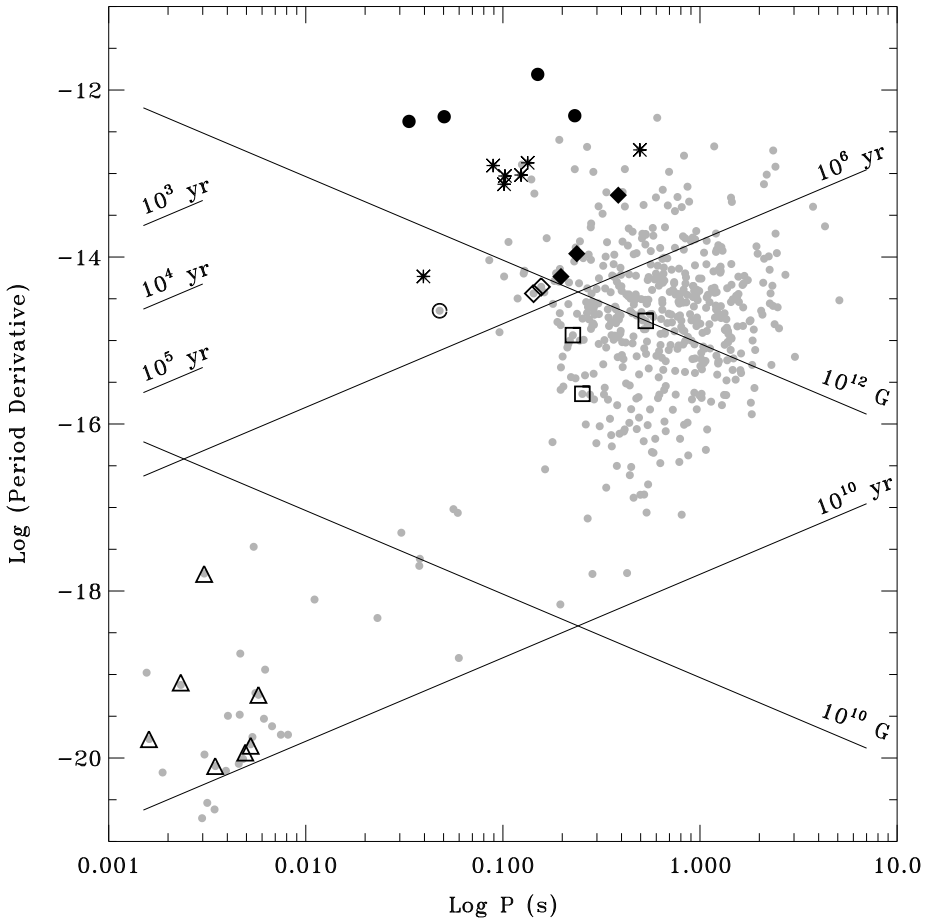

Fig. 1. The sample of rotation-powered pulsars plotted with respect to their spin parameters $P, \dot{P}$. Separate from the majority of ordinary field pulsars are the millisecond pulsars in the lower left corner. X-ray detected pulsars are indicated by symbols defined in Fig.4. Lines representing constant ages $\tau = P/2\dot{P}$ and magnetic field strength $B_\perp = 3.3 \times 10^{19}(P\dot{P})^{1/2}$ are indicated.

2. Data analysis

The observational data have been reviewed recently by Ögelman (1995), Trümper (1995) and Becker (1995a,b). However, most of the spectra and luminosities were collected from the available literature, resulting in a rather inhomogeneous data set. Actually, the quoted soft X-ray luminosity depends strongly on the detector type (the PSPC has limited spectral resolution, the HRI none), spectral model, distance model, absorption column and photon statistics. In this paper we present a homogeneous data set obtained by re-analyzing most of the ROSAT observations of pulsars in a standard way by making power-law and black-body fits to the count rate spectra using EXSAS (Zimmermann et al. 1994). The absorption columns N_H are deduced from spectral fits, or, if no detailed analysis was possible, from HI surveys (Dickey & Lockman 1990, Stark et al. 1992), from the optical extinction (cf. Becker et al. 1997b and references therein) or from the radio dispersion measure DM by assuming a mean electron density of $\bar{n}_e$ = 0.03 cm^{-3}. For the pulsar distances we used the model of Taylor & Cordes (1993) which *on average* yields distances correct up to a nominal error of about 25%. We used the proper motion corrected period derivatives to compute $\dot{E}$, $B_\perp$ and the spin-down age τ for all those pulsars for which this effect is of significance and has been measured (Camilo, Thorsett & Kulkarni 1994; Bell et al. 1995).

While our data analysis is done in a homogeneous way, the observational data differ significantly from source to source with respect to the total number of counts available and the energy range covered. Observational properties are summarized in Table 1. Sources for which a spectral analysis is meaningless for statistical reasons or which have been observed with the HRI only are labeled in the column *spectral info* with *no*. It turns out that with the exception of the younger pulsars (Crab, PSR 1509-58 and Vela) all measured pulse-phase averaged photon indices are consistent with $\alpha \approx -2$ (cf. Fig. 2). Therefore in calculating luminosities of the power-law components we used the individual photon indices given in Table 2 and a *canonical* value of $\alpha = -2$ where no spectral information was available.

The energy fluxes f_x within the 0.1-2.4 keV band have been converted to isotropic luminosities using $L_x = 4\pi d^2 f_x$. The X-ray luminosities for the total pulsar emission (L_x^{tot}), a pulsed component if detected (L_x^{puls}) and for the pulsar plus nebula (L_x^{pn}) if a nebula has been identified, are given in Table 3. We further give there the bolometric luminosities (L_{bol}^{∞}) for the black-body component of Geminga, PSR 0656+14 and 1055-52 (which in the following we will call *the three musketeers*) and upper limits for the other pulsars assuming a neutron star with a medium stiff equation of state (FP-Model, M = 1.4 M$_\odot$ and R = 10.85 km). In Table 3 the sources are ordered according to $\dot{E}/4\ \pi\ d^2$ down to $\sim 1.5 \times 10^{-11}$ erg s^{-1}cm^{-2}. The Princeton

Table 1. List of observational properties of the X-ray detected rotation-powered pulsars, ordered according to $\dot{E}/4\pi d^2$. The individual columns are as follows: 1. Pulsar name, 2. column density in units of 10^{21} cm^{-2}, 3. energy range in which the soft X-rays have been detected with ROSAT, 4. background and vignetting corrected count rate after cleaning the data for solar scattered X-rays and the particle background contribution. P,H indicates PSPC and HRI, respectively, 5. spectral information; pwl: power-law, bb: black-body spectrum. For PSR 0656+14 and PSR 1055-52 the photon-index of the power-law spectrum has to be fixed to yield good spectral fits with the compound black-body and power-law model. We fixed it to $\alpha = -2$. *PSR 1259−63 was observed at an orbital phase angle of $\sim 13^\circ$ post-apastron. Ref: [tw]this work, [1]Ögelman (1995), [2]Halpern & Ruderman (1993), [3]Becker, Brazier & Trümper (1995), [4]Safi-Harb, Ögelman & Finley (1995), [5]Finley & Srinivasan (1996), [6]Finley & Ögelman (1994), [7]Yancopoulos, Hamilton & Helfand (1994), [8]Becker et al. (1997b), [9]Danner, Kulkarni & Thorsett (1994), [10]Finley et al. (1993), [11]Manning & Willmore (1993), [12]Kawai & Tamura (1997), [13]Halpern (1996), [14]Becker, Brazier & Trümper (1996), [15]Verbunt et al. (1996), [16]Becker et al. (1996).

Pulsar	N_H $[10^{21} cm^{-2}]$	observed in range [KeV]	count rate in total band [cts/s]	spectral info	Ref.
B0531 + 21	~ 3	$0.5-2.4$	H:17.8 ± 0.05	pwl	tw
B0833 − 45	0.4 ± 0.1	$0.1-2.4$	P: 3.4 ± 0.02	pwl or bb	tw,1
B0633 + 17	0.1 ± 0.04	$0.1-2.4$	P: $5.4 \pm 0.3 \times 10^{-1}$	bb+pwl	tw,2
B1706 − 44	~ 5.4	$0.5-2.4$	P: $2.2 \pm 0.2 \times 10^{-2}$	pwl	3
B1509 − 58	~ 8	$0.5-2.4$	H: $3.6 \pm 0.1 \times 10^{-3}$	pwl	tw
B1951 + 32	3.4 ± 1.5	$0.5-2.4$	P: $6.8 \pm 0.3 \times 10^{-2}$	pwl	tw,4
B1046 − 58	~ 4	$0.5-2.4$	H: $2.3 \pm 0.4 \times 10^{-3}$	no	tw
B1259 − 63*	3.6 ± 0.5	$0.5-2.4$	P: $3.0 \pm 0.1 \times 10^{-2}$	pwl	tw
B1823 − 13	~ 8.2	$0.5-2.4$	P: $8.6 \pm 0.1 \times 10^{-3}$	no	tw,5
B1800 − 21	~ 14	$0.5-2.4$	P: $1.5 \pm 0.5 \times 10^{-3}$	no	tw,6
B1929 + 10	0.8 ± 0.3	$0.5-2.4$	P: $1.17 \pm 0.07 \times 10^{-2}$	pwl or bb	tw,7
J0437 − 47	0.08 ± 0.02	$0.1-2.4$	P: $2.04 \pm 0.06 \times 10^{-1}$	pwl	tw,8
B1821 − 24	~ 3	$0.5-2.4$	P: $1.0 \pm 0.2 \times 10^{-2}$	ASCA,pwl	tw,9
B0656 + 14	0.06 ± 0.01	$0.1-2.4$	P: 1.92 ± 0.03	bb+pwl(fixed)	tw
B0540 − 69	4(+0.6; −0.4)	$0.5-2.4$	H: $3.7 \pm 0.1 \times 10^{-2}$	pwl	tw,10
J2124 − 33	$0.2-0.5$	$0.1-2.4$	H: $2.6 \pm 0.2 \times 10^{-3}$	no	tw,8
B1957 + 20	~ 4.5	$0.5-2.4$	P: $4.2 \pm 0.6 \times 10^{-3}$	no	tw
B0950 + 08	~ 0.17	$0.1-2.4$	P: $4.9 \pm 0.9 \times 10^{-3}$	no	tw,11
B1610 − 50				ASCA,no	12
J0538 + 28	~ 1.2	$0.5-2.4$	P: $6.0 \pm 0.1 \times 10^{-2}$	no	tw
J1012 + 53	~ 0.07	$0.1-2.4$	P: $5.5 \pm 2.0 \times 10^{-3}$	no	tw,13
B1055 − 52	0.33 ± 0.1	$0.1-2.4$	P: $3.51 \pm 0.05 \times 10^{-1}$	bb+pwl(fixed)	tw
B0355 + 54	~ 1.8	$0.5-2.4$	P: $4.0 \pm 1.4 \times 10^{-3}$	no	tw
B2334 + 61	~ 3	$0.5-2.4$	P: $1.8 \pm 0.5 \times 10^{-3}$	no	tw,14
J0218 + 42	~ 0.5	$0.1-2.4$	H: $2.1 \pm 0.4 \times 10^{-3}$	no	tw,15
B0823 + 26	~ 0.4	$0.1-2.4$	P: $1.6 \pm 0.4 \times 10^{-3}$	no	tw
J0751 + 18	~ 0.44	$0.1-2.4$	P: $3.6 \pm 0.6 \times 10^{-3}$	no	tw,16

pulsar archive (Taylor et al. 1995) contains 71 pulsars above this limit, including 45 objects which have not been detected in X-rays yet[1]. 12 of them have been observed by ROSAT in pointed observations but were not detected while 10 were in the ROSAT field of view serendipitously. We have derived 1σ upper limits for 19 of the 22 pulsars applying the procedure described above. The corresponding upper limits for their luminosity are given in Table 4 and in Fig.4, which we shall discuss later.

3. The X-ray emission properties of pulsars

Before taking a synoptic look at the sample of the 26 pulsars detected in the ROSAT band a few additional remarks on their X-ray emission characteristics are appropriate. To this end we group the whole sample into five classes:

3.1. The Crab-like pulsars

It is well established that in the young Crab-like pulsars with ages ≤ 2000 years magnetospheric emission dominates. In the case of the Crab pulsar, for example, at least $\sim 75\%$ of the total soft X-ray flux is magnetospheric emission (Becker & Aschenbach 1995) characterized by a power-law spectrum and sharp pulses. With the ROSAT HRI an upper limit for the unpulsed flux within the 0.1-2.4 keV range can be deduced from the DC level of the soft X-ray pulse profile. The latter can be taken as an upper limit for the thermal flux from the Crab pulsar which is marginally consistent with standard cooling models (Becker & Aschenbach 1995, cf. Fig.3). The same holds for PSR 1509-

[1] We note that one X-ray detected pulsar was not listed in the available version of the Princeton pulsar catalog.

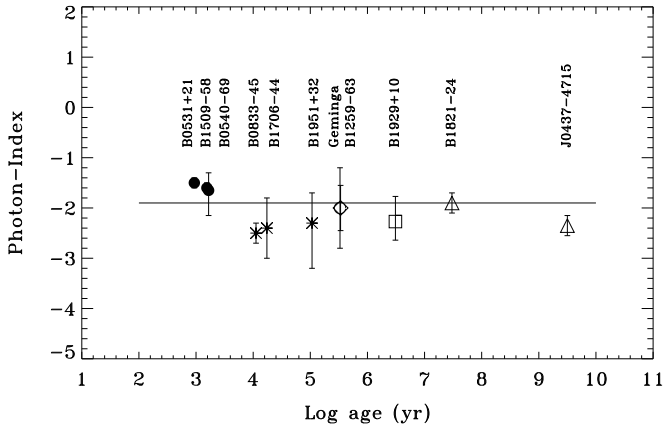

Fig. 2. The distribution of pulse-phase averaged photon indices vs. spin-down age for those pulsars which provides spectral information in the soft X-ray domain. The weighted mean of the photon indices is $\bar{\alpha} = -1.9 \pm 0.8$.

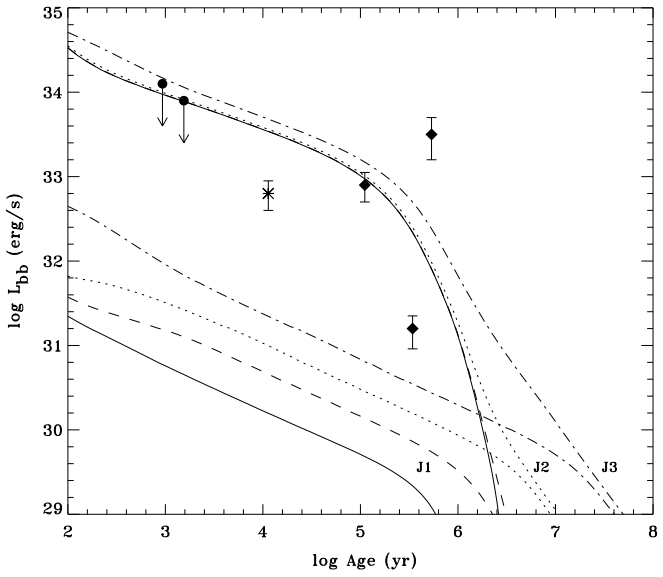

Fig. 3. Bolometric luminosities $L_{bol}^{\infty} = 4\,\pi\,d^2\,f_{bol}$ for the three musketeers (PSR 0656+14, Geminga and 1055-52) and the Vela pulsar as a function of the pulsar's characteristic age. Also shown are the upper limits for the Crab pulsar and PSR 1509-58 (cf. Table 3). Symbols are defined in Fig.4. For comparison, the cooling curves for standard and accelerated neutron star cooling (FP-Model) including frictional heating with strong (J3), weak (J2) and super-weak (J1) pinning of crustal superfluid vortex lines are shown (Umeda et al. 1993). We note that the given error bars indicate 1σ errors as obtained from spectral fits. Distance uncertainties which might contribute a much larger error are not taken into account.

Table 2. List of pulse-phase averaged photon-indices

Pulsar	α	Ref.
B0531 + 21	-1.5 ± 0.1	Toor & Seward (1977)
B1509 − 58	-1.6 ± 0.1	Kawai et al. (1992)
B0540 − 69	$-1.65^{+0.35}_{-0.5}$	Finley et al.(1993)
B0833 − 45*	-2.5 ± 0.2	this work
B1706 − 44	-2.4 ± 0.6	Becker et al. (1995)
B1951 + 32*	$-2.3^{+0.6}_{-0.9}$	this work
B1259 − 63**	-2.0 ± 0.8	this work
B0633 + 17	-2.0 ± 0.45	this work
B1929 + 10	$-2.27^{+0.5}_{-0.37}$	this work
B1821 − 24	-1.9 ± 0.2	Saito et al.(1997)
J0437 − 47	-2.35 ± 0.2	Becker et al. (1997b)

*Photons from within a 35" circle centered on the pulsar.
** Observed at 13° post-apastron.

58 which from our ROSAT HRI observation is found to have a pulsed fraction of $65 \pm 4\%$ (Becker et al. 1997a) and a soft X-ray pulse which is aligned with the hard pulses detected at $20 - 170$ keV by BATSE and OSSE (Ulmer et al. 1994). The pulsar's count rate deduced from the DC-level of the soft X-ray light curve can be taken as an upper limit for the thermal flux (cf. Table 3 and Fig.3).

3.2. The Vela-type pulsars

Different from the Crab-like pulsars are pulsars in the age bracket $\sim 10^4 - 10^5$ years (e.g. the Vela-pulsar, PSR 1706-44, 1046-58, 1800-21, 1823-13 and 1951+32). They exhibit strong steady emission from a pulsar-powered synchrotron nebula combined with a small pulsed contribution of magnetospheric or thermal origin dominating the emission in the range $\sim 0.1 - 0.5$ keV (Ögelman, Finley & Zimmerman 1993; Becker & Trümper 1996). X-ray pulses are only detected for the Vela pulsar. The other Vela-type pulsars are more distant and suffer from photoelectric absorption which prevents the detection of their soft pulses in the presence of the dominant nebula emission (Becker & Trümper 1996). Apart from the Vela pulsar itself there is no spectral information for this sources below 0.5 keV (cf. Table 1) which means that their black-body component is invisible because of photoelectric absorption.

3.3. The cooling neutron stars

Our analysis confirms the results obtained earlier by several authors (e.g. Ögelman & Finley 1993; Becker et al. 1993; Mereghetti & Colpi 1996; Halpern & Wang 1997) on the three middle age pulsars Geminga, PSR 0656+14 and 1055-52. The X-ray emission properties of these pulsars are characterized by a dichotomy, i.e. the spectra are best described by a two-component model in which the soft emission is represented by a black-body spectrum and the hard component either by a thermal spectrum or by a power-law. The existence of two spectral components is also confirmed by phase-resolved analysis. All three pulsars show a phase shift of $\sim 100°$ and a change in the pulsed fraction from $\sim 10 - 30\%$ below a transition point of $0.5 - 0.6$ keV, rising up to $\sim 20 - 65\%$ above. The X-ray pulse profile for both the soft and the hard components is found to be sinusoidal.

Table 3. List of pulsars that have been detected in the radio, optical, X- and γ-ray wavebands, ordered according to their spin-down flux density at Earth $\dot{E}/4\pi d^2$. The individual columns are as follows: 1. Pulsar name; 2-7. Energy ranges in which pulsed (p), unpulsed (d) radiation has been detected: R – radio, O – optical, X_s – soft X-rays ($E_\gamma \sim$ 1keV), X_h – hard X-rays ($E_\gamma \sim$ 10keV), γ_s – soft γ-rays ($E_\gamma \sim$ 1MeV) and γ_h – hard γ-rays ($E_\gamma >$ 100MeV). Possible detections are indicated by a question mark. lg $\dot{E}$ is the pulsar spin-down power $I\Omega\dot{\Omega}$; L_x^{tot} the sum of the pulsed and unpulsed X-ray luminosities assuming isotropic emission. L_x^{puls} is the pulsed luminosity; L_x^{pn} is the total X-ray luminosity including synchrotron nebula emission. All luminosities are calculated for the ROSAT energy range $0.1 - 2.4$ keV. For Geminga, PSR 0656+14 and 1055-52 thermal and non-thermal contributions are included. lg L_{bol}^{∞} is the bolometric luminosity. The upper limits have been computed for a neutron star with a medium stiff equation of state (FP-Model, M = 1.4 $M_\odot$ and R = 10.85 km). *PSR 1259-63 was observed $\sim 13^\circ$ post-apastron. Ref: ^{tw}this work, [1]Becker & Aschenbach (1995), [2]Ögelman (1995), [3]Becker, Brazier & Trümper (1995), [4]Becker et al.(1997a), [5]Becker & Trümper (1993), [6]Finley et al.(1993), [7]Becker et al.(1997b), [8] Kawai & Tamura (1996), [9]Becker, Brazier & Trümper (1996), [10]Becker et al.(1996). Radio pulsar parameters have been taken from Taylor et al. (1995). Proper motion corrected period derivatives have been used for all those pulsars for which this effect is of significance and has been measured. A summary of the optical and γ-ray observations can be found in Caraveo (1995) and Thompson (1996), respectively. For a possible detection of PSR 0950+08 at optical wave length see Pavlov, Stringfellow & Córdova (1996).

Characteristics of the optical, X-ray and gamma-ray detected rotation-powered pulsars

Pulsar	Comment	detected						$\dot{E}/(4\pi d^2)$	lg $\dot{E}$	lg L_x^{tot}	lg L_x^{puls}	lg L_x^{pn}	lg L_{bol}^{∞}	lg$(P/2\dot{P})$	P	$\dot{P} \times 10^{-15}$	D	lg $B_\perp$	Ref.
		R	O	X_s	X_h	γ_s	γ_h	erg/s/cm^2	erg/s	erg/s	erg/s	erg/s	erg/s	years	ms	s s^{-1}	kpc	Gauss	
B0531 + 21	Crab	p	p	p	p	p	p	$9.3 \cdot 10^{-7}$	38.65	35.98	35.85	37.3	$\leq$ 34.1	3.10	33.40	420.96	2.00	12.58	1
B0833 − 45	Vela	p	p	p	p	p	p	$2.3 \cdot 10^{-7}$	36.84	32.70	31.7	33.4	$\sim$ 32.8	4.05	89.29	124.68	0.50	12.53	tw,2
B0633 + 17	Geminga	?	d	p	-	-	p	$1.1 \cdot 10^{-8}$	34.51	31.10	30.62		31.2	5.53	237.09	10.97	0.16	12.21	tw
B1706 − 44	G343.1-02.3	p	-	d	-	-	p	$8.6 \cdot 10^{-9}$	36.53	33.15			$\leq$ 33.5	4.24	102.45	93.04	1.82	12.49	3
B1509 − 58	MSH 15-52	p	d	p	p	p	-	$7.7 \cdot 10^{-9}$	37.25	34.29	34.10	35.3	$\leq$ 33.9	3.19	150.23	1540.19	4.30	13.19	tw,4
B1951 + 32	CTB 80	p	-	d	-	-	p	$5.0 \cdot 10^{-9}$	36.57	33.44		34.0	$\leq$ 33.9	5.03	39.53	5.85	2.50	11.69	tw
B1046 − 58	Vela twin	p	-	d	-	-	?	$1.9 \cdot 10^{-9}$	36.30	32.64			$\leq$ 33.4	4.31	123.65	95.92	2.98	12.54	tw
B1259 − 63*	Be-star/bin	p	-	d	d	d	-	$1.7 \cdot 10^{-9}$	35.92	32.95			$\leq$ 33.8	5.52	47.76	2.27	2.00	11.51	tw
B1823 − 13	Vela like	p	-	d	-	-	-	$1.4 \cdot 10^{-9}$	36.45	33.39			$\leq$ 33.9	4.33	101.45	74.95	4.12	12.45	tw
B1800 − 21	G8.7-0.1	p	-	d	-	-	-	$1.2 \cdot 10^{-9}$	36.35	33.06			$\leq$ 33.8	4.30	133.61	134.32	3.94	12.63	tw
B1929 + 10		p	d	p	-	-	-	$1.1 \cdot 10^{-9}$	33.59	30.00	29.5		$\leq$ 31.4	6.49	226.51	1.16	0.17	11.71	tw
J0437 − 47	ms Pulsar	p	-	p	-	-	-	$1.0 \cdot 10^{-9}$	33.62	30.86	30.3		$\leq$ 31.2	9.50	5.75	$2.0 \cdot 10^{-5}$	0.18	8.54	tw,5
B1821 − 24	ms,in M28	p	-	p	p	-	-	$6.2 \cdot 10^{-10}$	36.35	33.24			$\leq$ 33.7	7.48	3.05	$1.6 \cdot 10^{-3}$	5.50	9.35	tw
B0656 + 14	cooling NS	p	p	p	-	-	?	$5.5 \cdot 10^{-10}$	34.58	32.98	32.15		32.9	5.05	384.87	55.03	0.76	12.67	tw,2
B0540 − 69	in LMC	p	p	p	-	-	-	$5.1 \cdot 10^{-10}$	38.17	36.21	36.1	37.2	$\leq$ 36.1	3.22	50.37	479.06	49.4	12.70	6
J2124 − 33	ms Pulsar	p	-	p	-	-	-	$4.7 \cdot 10^{-10}$	33.55	30.35	29.8		$\leq$ 31.1	9.86	4.93	$1.08 \cdot 10^{-5}$	0.25	8.36	tw,7
B1957 + 20	ms Pulsar	p	-	d	-	-	-	$4.1 \cdot 10^{-10}$	35.06	31.93			$\leq$ 32.9	9.32	1.60	$1.2 \cdot 10^{-5}$	1.53	8.14	tw
B0950 + 08		p	?	d	-	-	-	$3.3 \cdot 10^{-10}$	32.75	29.35			$\leq$ 31.0	7.24	253.06	0.23	0.12	11.39	tw
B1610 − 50	ASCA	p	-	d	-	-	-	$2.5 \cdot 10^{-10}$	36.20					3.87	231.60	492.54	7.26	13.03	8
J0538 + 28	G180.0-1.7	p	-	d	-	-	-	$1.3 \cdot 10^{-10}$	34.69	32.74			$\leq$ 33.6	5.79	143.15	3.66	1.50	11.87	tw
J1012 + 53	ms Pulsar	p	-	d	-	-	-	$1.2 \cdot 10^{-10}$	33.60	30.20			$\leq$ 30.8	9.76	5.25	$1.4 \cdot 10^{-5}$	0.52	8.45	tw
B1055 − 52	cooling NS	p	d	p	-	-	p	$1.1 \cdot 10^{-10}$	34.48	33.42	32.57		33.5	5.73	197.10	5.83	1.53	12.03	tw,2
B0355 + 54		p	-	d	-	-	-	$8.8 \cdot 10^{-11}$	34.66	31.96			$\leq$ 33.8	5.75	156.38	4.39	2.07	11.92	tw
B2334 + 61	G114.3+0.3	p	-	d	-	-	-	$8.6 \cdot 10^{-11}$	34.79	31.86			$\leq$ 33.4	4.61	495.24	191.91	2.46	12.99	tw,9
J0218 + 42	ms Pulsar	p	-	d	-	-	-	$6.5 \cdot 10^{-11}$	35.39	32.75			$\leq$ 33.1	8.66	2.32	$8.0 \cdot 10^{-5}$	5.70	8.63	tw
B0823 + 26		p	-	d	-	-	-	$2.6 \cdot 10^{-11}$	32.66	29.83			$\leq$ 31.0	6.69	530.66	1.72	0.38	11.99	tw
J0751 + 18	ms Pulsar	p	-	d	-	-	-	$1.5 \cdot 10^{-11}$	33.88	31.60			$\leq$ 32.2	9.84	3.47	$8.0 \cdot 10^{-6}$	2.02	8.23	tw,10

Table 4. List of undetected pulsars observed in pointed and serendipitous ROSAT observations, ordered according to $\dot{E}/4\pi d^2$. The individual columns are as follows: 1. Pulsar name, 2-10. the pulsar's spin-down flux density at earth, its braking energy, characteristic age, period and period derivative, distance and magnetic dipole component, column density from dispersion measure and count rate upper limits. P,H indicates PSPC and HRI, respectively, 11. X-ray luminosity within 0.1-2.4 keV, assuming isotropic emission. We note that for PSR 1820-30A, 1356-60 and 1754-24 the data quality wasn't sufficient to deduce a useful upper limit (e.g. source located at the edge of the detector's field of view with an exposure time of less than a kilosecond).

Pulsar	$\dot{E}/(4\pi d^2)$ erg/s/cm^2	lg $\dot{E}$ erg/s	lg$(P/2\dot{P})$ years	P ms	$\dot{P} \times 10^{-15}$ s s^{-1}	D kpc	lg $B_\perp$ Gauss	N_H $10^{21} cm^{-2}$	count rate cts/s	L_x erg/s
B1757 − 24	$1.1 \cdot 10^{-9}$	36.41	4.19	124.87	127.89	4.61	12.61	~ 9.2	H: ≤ 0.0014	≤ 33.17
B1937 + 21	$7.1 \cdot 10^{-10}$	36.04	8.37	1.557	1.1 E-4	3.60	8.61	0.28 - 2.2	H: ≤ 0.0007	≤ 32.10
B1727 − 33	$5.8 \cdot 10^{-10}$	36.09	4.42	139.45	85.00	4.24	12.54	~ 7.9	P: ≤ 0.0020	≤ 32.73
B1257 + 12	$4.1 \cdot 10^{-10}$	33.73	9.50	6.22	3.3E-5	0.62	8.66	~ 3.2	P: ≤ 0.0011	≤ 29.99
B0114 + 58	$4.0 \cdot 10^{-10}$	35.34	5.44	101.44	5.84	2.14	11.89	~ 1.5	P: ≤ 0.0033	≤ 31.84
B0740 − 28	$3.4 \cdot 10^{-10}$	35.16	5.20	166.76	16.811	7.80	12.23	~ 2.0	P: ≤ 0.0020	≤ 32.79
B1853 + 01	$3.3 \cdot 10^{-10}$	35.63	4.31	267.40	208.40	3.30	12.88	~ 3.0	H: ≤ 0.0022	≤ 32.63
B1830 − 08	$1.5 \cdot 10^{-10}$	35.77	5.17	85.28	9.17	5.67	11.95	~ 12.6	P: ≤ 0.0017	≤ 33.16
B1820 − 30A	$1.1 \cdot 10^{-10}$	35.92	7.41	5.44	3.3E-3	8.00	9.64	~ 2.7		
J1908 + 07	$8.4 \cdot 10^{-11}$	33.53	6.61	212.35	8.25E-1	0.58	11.63	~ 0.34	P: ≤ 0.0045	≤ 30.57
B1737 − 30	$6.4 \cdot 10^{-11}$	34.91	4.32	606.69	465.30	3.28	13.23	4.7 - 9.5	P: ≤ 0.0023	≤ 32.36
B1620 − 26	$5.9 \cdot 10^{-11}$	34.36	8.35	11.07	7.90E-4	1.80	9.48	~ 1.9	P: ≤ 0.0010	≤ 31.66
J2322 + 20	$4.8 \cdot 10^{-11}$	33.15	10.32	4.80	4E-6	0.78	8.11	~ 0.4	P: ≤ 0.0006	≤ 29.99
J2019 + 24	$4.6 \cdot 10^{-11}$	33.11	10.43	3.93	2E-6	0.91	8.00	~ 0.5	P: ≤ 0.0007	≤ 30.25
B1822 − 09	$3.7 \cdot 10^{-11}$	33.66	5.37	768.98	52.36	1.01	12.81	~ 0.6	P: ≤ 0.0014	≤ 30.65
J0631 + 10	$3.4 \cdot 10^{-11}$	35.24	4.64	287.75	104.62	6.56	12.74	~ 3.9	P: ≤ 0.0051	≤ 33.23
B1534 + 12	$3.2 \cdot 10^{-11}$	33.24	8.30	37.90	2.4E-3	0.68	9.98	~ 0.4	P: ≤ 0.0019	≤ 30.35
B1356 − 60	$2.9 \cdot 10^{-11}$	35.08	5.50	127.50	6.33	5.91	11.96	~ 9.1		
B1754 − 24	$2.7 \cdot 10^{-11}$	34.60	5.46	234.09	13.00	3.50	12.25	~ 5.5		
B0611 + 22	$2.4 \cdot 10^{-11}$	34.80	4.95	334.92	59.63	4.72	12.65	~ 3.0	P: ≤ 0.0011	≤ 32.20
B1828 − 10	$2.3 \cdot 10^{-11}$	34.55	5.03	405.03	60.04	3.63	12.70	~ 5.0	P: ≤ 0.0022	≤ 32.24
B1742 − 30	$1.6 \cdot 10^{-11}$	33.93	5.74	367.43	10.66	2.08	12.30	~ 2.7	P: ≤ 0.0007	≤ 31.18

The soft thermal emission is assigned to be cooling emission from the neutron star's surface. The modulation of this emission can be explained by non-uniformities in the surface temperature due to the presence of a strong magnetic field which gives rise to an anisotropic heat flow in the neutron star's outer layers. The radius of the emitting area obtained by using $R_{bb} = d/T^2 \sqrt{f_{bol}/\sigma}$, in which f_{bol} and T denotes the fitted bolometric flux and temperature of the pulsar's soft component and σ the Stefan-Boltzmann constant, are found to be close to the canonical neutron star radius of 10 km.

The hard spectral components of these pulsars can be interpreted as magnetospheric emission or thermal radiation from polar hot spots. Because of bandwidth limitations a distinction between these possibilities cannot be made on the basis of ROSAT PSPC spectra. But ASCA observations have shown recently that the hard component of Geminga is characterized by a power-law implying a magnetospheric origin (Halpern & Wang 1997). Similar results have been reported for PSR 0656+14 and 1055-52 (Greiveldinger et al. 1996), although the limited photon statistics in these cases prevent a clear distinction between a thermal and non-thermal origin of the emission.

In Fig. 3 we have plotted the bolometric black-body luminosities $L_{bol}^{\infty} = 4\,\pi\,d^2\,f_{bol}$ for the three musketeers and Vela as obtained from spectral fits. The figure demonstrates that the thermal emission from PSR 0656+14 and PSR 1055-52 is consistent with the prediction of standard cooling for a neutron stars with a medium stiff equation of state, while Vela and Geminga are located below the standard cooling curves.

We note that for the three musketeers optical (Pavlov, Stringfellow & Cordova 1996; Mignani, Caraveo & Bignami 1997a; Shearer et al. 1996a) and for Geminga and PSR 0656+14 EUV emissions have been found (PSR 1055-52 has not yet been observed in the EUV regime). The ROSAT and EUVE spectra can be fitted by a single modified black-body component using photospheric opacities (Zavlin et al. 1995). In the case of Geminga the optical emission lies close to the Rayleigh-Jeans extrapolation of the X-ray/EUV spectrum while for PSR 0656+14 and PSR 1055-52 the optical flux is higher than that by about one order of magnitude (Shearer et al. 1996b; Mignani, Caraveo & Bignami 1997b, Kurt et al. 1997). In Geminga an optical emission feature was reported at ~ 6000 Å (Bignami et al. 1996) which has been attributed to proton cyclotron emission from a photospheric plasma.

Besides PSR 0656+14, Geminga and PSR 1055-52 two more pulsars are classified as cooling neutron stars: PSR 0538+28 and 0355+54. Both have spin parameters similar to the one observed for Geminga and 1055-52 and both appear to be good candidates for gamma-ray pulsars. However, the sources

are approximately a factor of 10 more distant than Geminga and the limited photon statistics did not allow a spectral or temporal analysis so that their classification is not yet based on X-ray observations.

The three cooling neutron star candidates located in the supernova remnants RCW 103, PKS 1209-51/52 and Puppis A (cf. Caraveo, Bignami & Trümper 1996 and references therein) will not be considered here.

3.4. Pulsars old and close in space

Besides the young pulsars and those whose surface cooling is visible in the X-ray wave band, ROSAT has detected X-ray emission from further three pulsars: PSR 1929+10, 0950+08 and 0823+26. All are characterized by a spin-down age of $\sim 0.2 - 3 \times 10^7$ years and a close distance of $\sim 0.12 - 0.38$ kpc. Pulsed X-ray emission, however, could only be detected from PSR 1929+10 (Yancopoulos, Hamilton & Helfand 1994). Its X-ray pulse profile is very broad with a single pulse stretching across almost the entire phase cycle. Spectral information is only available for 1929+10. We found that both a power-law and a black-body spectrum fits the data equally well. The results of our spectral fits are given in Table 1−3.

3.5. The millisecond pulsars

The millisecond pulsars form a separate group among the rotation-powered pulsars. They are distinguished by their small spin periods ($P \leq 20$ ms) and high rotational stability ($dP/dt \approx 10^{-18} - 10^{-21}$) and, consequently, they are very old objects with spin-down ages of typically $10^9 - 10^{10}$ years and magnetic field strengths of the order of $10^8 - 10^{10}$ G. Before ROSAT nothing was known about the X-ray emission properties of this class of pulsars. Their location in the $L_x - \tau$ diagram (cf. Fig.5) had initially led to the suggestion that their radiation is a mixture of spin-modulated thermal emission from heated polar caps possibly combined with unpulsed emission from a pulsar wind or a plerion (Becker & Trümper 1993). The PSPC spectrum of PSR J0437−4715 can be fitted by a power-law with a photon-index of ≈ -2.4. A feature in the energy dependent pulsed fraction of this source which had been interpreted as evidence for an additional weak thermal component (Becker & Trümper 1993) has disappeared in the present reanalysis (Becker et al. 1997b). Recent ASCA observations of the millisecond pulsar PSR 1821-24 in M28 led to the detection of X-ray pulses up to 10 keV (Saito et al. 1997). The spectrum is a power-law with a pulse-phase averaged photon-index of ≈ -2, indicative of magnetospheric emission. The recent discovery of pulsed soft X-rays from the isolated millisecond pulsar PSR J2124-3358 (Becker et al. 1997b) which has spin parameters similar to that of PSR J0437-4715 and a pulse profile similar to the one observed in the radio channel at 480 MHz (Bailes et al. 1997) strongly suggests that the X-ray emission of millisecond pulsars is of magnetospheric origin. The next paragraph will further support this interpretation.

4. Synoptic view and discussion

Fig. 4 shows the X-ray luminosities of all 26 pulsars measured in the ROSAT band as a function of their rotational energy loss $\dot{E}$. We note that the young but distant pulsar PSR 1610-50 has not yet been observed by ROSAT and the sparse ASCA data provide only a rough flux estimate (Kawai, Tamura & Shibata 1996) so that we have excluded this source from our analysis. In the case of the *three musketeers* we have plotted the luminosities derived for the power-law component (i.e. $\log L_x$ = 30.06, 31.58, 31.88 erg/s for Geminga, PSR 0656+14 and 1055-52, respectively).

Fig.4 shows a rather close linear correlation between the X-ray luminosity and the spin-down power. Fitting a $L_x(0.1 - 2.4 \text{ keV}) = a\ \dot{E}^b$ distribution to the data we find $b = 1.03 \pm 0.08$ and a correlation coefficient of $r = 0.946$. We note that Seward & Wang (1988) and Ögelman (1995) found for much smaller samples $b = 1.39$ and $b = 1.35 \pm 0.25$ respectively, which does not deviate significantly from our value (cf. also Possenti, Mereghetti & Stella 1996). Adopting $b = 1$ the efficiency of conversion is $\eta_x = L_x/\dot{E} = 10^{-3}$ for the X-rays in the ROSAT band, indicated by the dashed-line in Fig.4.

It is remarkable how narrow the $L_x(\dot{E})$ distribution is in view of the various effects which are expected to widen it: uncertainties in the pulsar distances and the absorption column N_H, spread in the orientations of magnetic and rotational axes versus the line of sight and spread in the moments of inertia. These effects are expected to account for a large fraction of the scatter leaving little room for *intrinsic fluctuations* of the X-ray efficiency.

The strong correlation suggests that the prime energy source of the X-ray emission is the pulsar's rotational energy. The conversion into X-rays can proceed via different channels: (1) magnetospheric processes or (2) emission from hot spots which both produce pulsed X-rays, (3) pulsar wind or synchrotron nebular emission which lead to unpulsed X-rays. In view of the fact that pulsed emission has been measured for only 11 of the 26 pulsars (cf. Table 3) and unpulsed components may not be spatially resolved because of limited angular resolution (and photon statistics) it is difficult to assess the relative importance of the different emission processes.

But in particular the millisecond pulsars showing pulsed emission obey the same linear relationship with the same X-ray efficiency as the Crab type pulsars. This indicates that their emission is mainly due to magnetospheric processes in line with the occurrence of power-law spectra and the similarity of radio/X-ray pulse profiles as discussed in Sect. 3.5. We cannot exclude that some additional components from a polar hot spot contributes (cf. Zavlin & Pavlov 1997) but this cannot be the dominating component for most pulsars. Only for the three middle aged pulsars PSR 0656+14, Geminga and PSR 1055-52 and probably for the Vela-pulsar is an additional thermal component detected which can be attributed to photospheric emission from the neutron stellar surface.

Another way to look to the sample of the X-ray detected rotation-powered pulsars is shown in Fig. 5 where the X-ray luminosity in the ROSAT band is plotted as a function of the

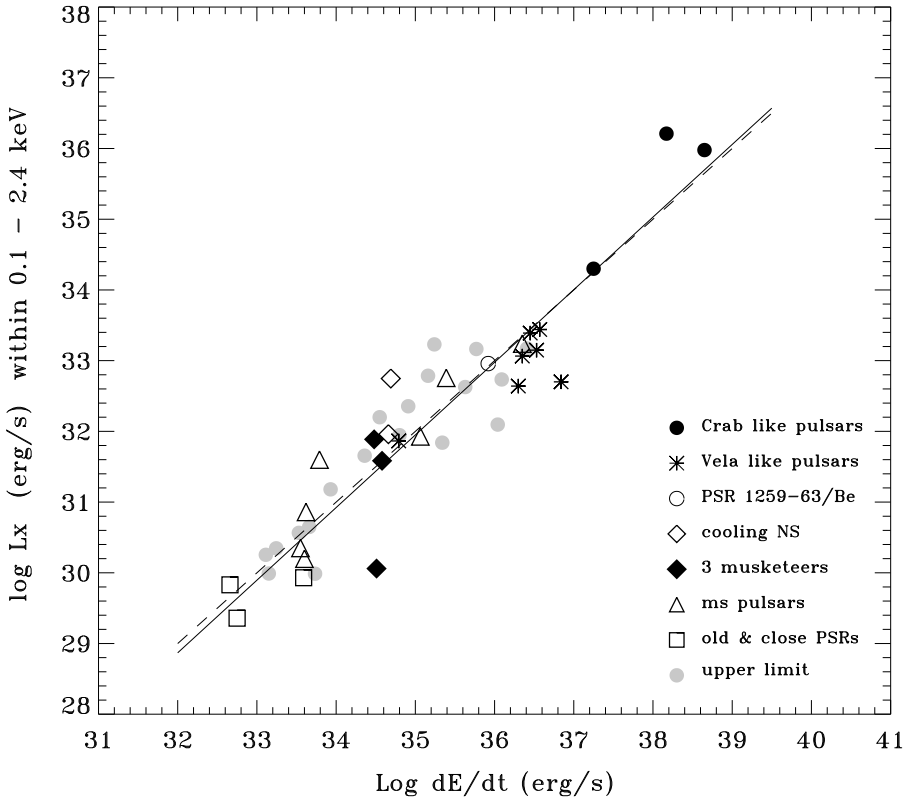

Fig. 4. X-ray luminosity vs. spin-down energy for all rotation-powered pulsar detected by ROSAT as of July 1997. We note that for the three musketeers Geminga, PSR 0656+14 and 1055-52 the low energy thermal component has been subtracted from the data. The solid line represents $L_x(\dot{E}) \propto \dot{E}^{1.03}$, the dashed line $L_x(\dot{E}) = 10^{-3} \times \dot{E}$. 1σ upper limits for the X-ray luminosity of all pulsars which have a $\dot{E}/4\pi d^2 \geq 1.5 \times 10^{-11}$ erg s^{-1}cm^{-2} and have been observed but were not detected in pointed and serendipitous ROSAT observations are indicated.

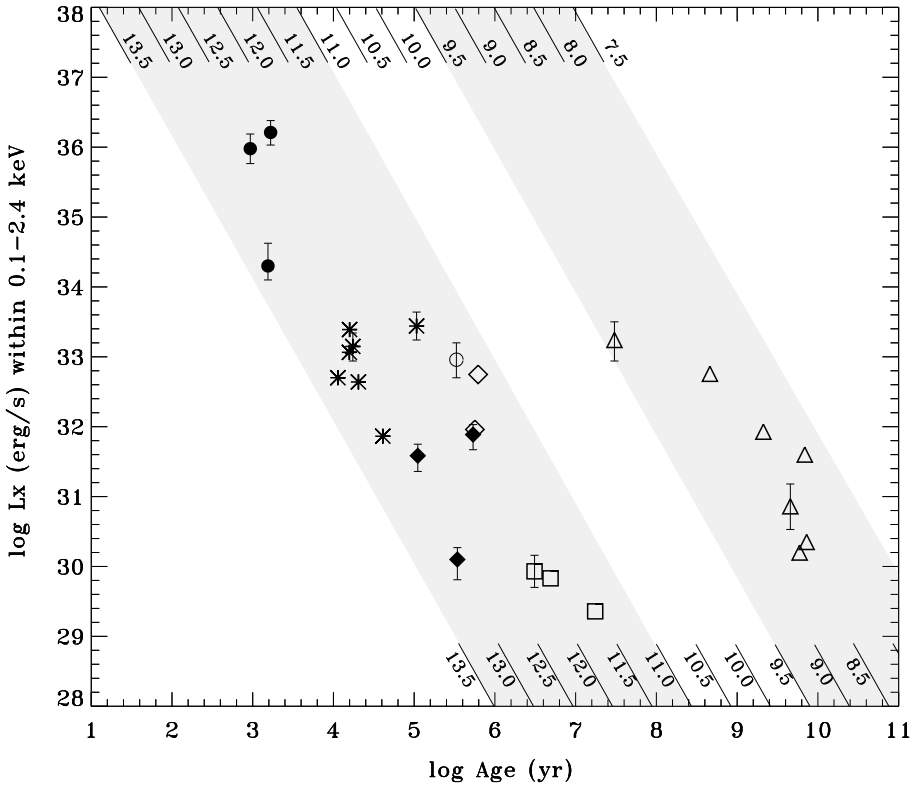

Fig. 5. X-ray luminosities of the ROSAT detected rotation-powered pulsars within $0.1 - 2.4$ keV as a function of the pulsar's characteristic age. The plotted luminosities have been derived from power-law spectra and can be attributed to magnetospheric emission. A thermal component as detected for the three musketeers and Vela has been subtracted. Curves corresponding to $L_x = \eta_x \dot{E}$ for $\log B_\perp = 7.5, \ldots, 13.5$ G are indicated. Symbols are defined in Fig.4.

pulsar's characteristic age. Assuming the standard picture of magnetic braking we can write

$$L_x = \eta_x \dot{E} \propto R^6 \, B_\perp^2 \, \Omega^4 \quad (1)$$

where $B_\perp$, R, and Ω are the polar magnetic field strength, radius and angular velocity of the neutron star, respectively. Using $I = 10^{45}$ g cm^2, $R = 10^6$ cm and making the standard assumption that the present angular velocity Ω is small compared with the initial one we find

$$L_x = \eta_x \dot{E} = const. \, B_\perp^{-2} \, \tau^{-2} \quad (2)$$

The corresponding $L_x(\tau)$ curves for different magnetic field strength are indicated in Fig.5. We note that all pulsars lie close to the braking curves calculated for their respective polar magnetic fields. Of course, this message is fully equivalent to that of Fig.4, namely that the X-ray luminosity is proportional to the rotational energy loss.

5. Conclusion

Although *ordinary field* pulsars and millisecond pulsars form well-separated populations in the $L_x(\tau)$ diagram they obey the same $L_x \propto \dot{E}$ correlation. The surprisingly close correlation between L_x and $\dot{E}$ strongly suggests that the bulk of the observed X-rays is emitted at the expense of rotational energy. The fact that the measured X-ray spectra show largely power-laws at $E \geq 0.5$ keV indicates that the main emission process is a magnetospheric one, just as in case of the radio and gamma ray emission.

It is an old question whether the incoherent high energy emission of pulsars originates in the co-rotating inner magnetosphere or near the light cylinder. In the latter case one expects an intensity dependence on the angular frequency $L_{inc} \propto \Omega^n$ with $n \geq 10$ (Beskin, Gurevich & Istomin 1993). This is due to the simple fact that the radiation from the light cylinder must depend on the total "particle luminosity" $L_p \sim B_\perp^2 \, \Omega^4$ and on the electric and magnetic fields at the light cylinder which scale with $\sim B_\perp \, \Omega^3$. Beskin, Gurevich & Istomin (1993), for example, find $L_{inc} \sim B_\perp^5 \, \Omega^{11}$. In contrast, we obtain $L_x \propto B_\perp^2 \, \Omega^4$, assuming the validity of magnetic braking. It thus appears that the bulk of the X-rays observed in the sample of 27 pulsars originates in the co-rotating magnetosphere, e.g. by Compton scattering processes (Trümper, Supper & Becker 1997).

Acknowledgements. The ROSAT project is supported by the Bundesministerium für Bildung, Wissenschaft, Forschung und Technologie (BMBW) and the Max-Planck-Society (MPG). We thank our colleagues from the MPE ROSAT group for their support. We acknowledge discussions with G.G. Pavlov and V.E. Zavlin as well as useful comments of the referee I. Grenier.

References

Arons, J., Tavani, M., 1993, ApJ, 403, 249
Bailes, M., et al. 1997, ApJ, 481, 386
Becker, W., Brazier, K.T.S., Trümper, J.,1993, A&A, 273, 421
Becker, W. & Trümper, J., 1993, Nat, 365, 528
Becker, W., 1995a, Ph.D. thesis, MPE-Report 260.
Becker, W., 1995b, in *The Annals of the 17th Texas Symposium on Relativistic Astrophysics and Cosmology*, eds Böhringer H., Morfill G., Trümper J., NY Acad. of Sc., Vol 759, p250
Becker, W., Aschenbach, B., 1995, in *The Lives of Neutron Stars* eds A. Alpar, U. Kilizóglu & J. van Paradijs, Kluwer Academic Publishers, p.47
Becker, W., Brazier, K.T.S., Trümper, J., 1995, A&A, 298, 528
Becker, W., Brazier K.T.S., Trümper, J., 1996, A&A, 306, 464
Becker, W., Trümper, J., Lundgreen, S.C., Cordes, J.M., Zepka, A.F., 1996, MNRAS, 282, L33
Becker, W., Trümper, J., 1996, A&AS, 120, C69
Becker, W., et al. 1997a, in preparation
Becker, W., Trümper, J., et al. 1997b, in preparation
Bell, J.F., Bailes, M., Manchester, R.N., Weisberg, J.M., and Lyne, A.G., 1995, ApJ, 440, L81
Beskin, V.S., Gurevich, A.V., Istomin, Ya. N., 1993, *Physics of the Pulsar Magnetosphere*, Cambridge University Press, ISBN 0-521-41746-5, p.293
Bignami, G.F., Caraveo, P.A., Mignani, R., Edelstein, J., Bowyer, S., 1996, ApJ, 456, L111
Camilo, F., Thorsett, S.E., Kulkarni, S.R., 1994, ApJ, 421, L15
Caraveo, P.A., 1995, in *The Annals of the 17th Texas Symposium on Relativistic Astrophysics and Cosmology*, eds Böhringer H., Morfill G., Trümper J., NY Acad. of Sc., Vol 759, p246
Caraveo, P.A., Bignami, G.F., Trümper, J., 1996, AA Rev. 7, 209
Cheng, K.S., Ho, C. & Ruderman, M.A., 1986a, ApJ, 300, 500
Danner, R., Kulkarni, S.R., Thorsett, S.E., 1994, ApJ436, L153
Dickey, J. M., Lockman, F. J., 1990, ARA & A., 28,215.
Finley, J.P., Ögelman, H., Hasinger, G., Trümper, J., 1993, ApJ, 410, 323
Finley, J.P., Ögelman, H., 1994, ApJ, 434, L25
Finley, J.P., Srinivasan, R. Park, S., 1996, ApJ, 466, 938
Gil, J.A., Krawczyk, A., 1996, MNRAS, 285, 566
Greenstein G., Hartke, G.J., 1983, ApJ, 271, 283
Greiveldinger, C., Camerini, U., Markwardt, C.B. et al., 1996, ApJ, 465, L35
Halpern, J., Ruderman, M., ApJ, 415, 286
Halpern, J., 1996, ApJL, 459, L9
Halpern, J.P., Wang, F.Y.-H., 1997, ApJ, 477, 905
Johnston, S., Walker, M.A., Bailes, M., 1996, *IAU Colloquium 160*, A.S.P Conference Series, Vol. 105
Kawai, N., Okayasu, R., Sekimoto, Y., 1992, in *AIP Conference Proceedings 280*, eds M.Friedlander, N.Gehrels & D.J. Macomb, St. Louis, Mo, p213
Kawai, N., Tamura, K., 1996, in *IAU Colloquium 160*, eds S.Johnston, M.A.Walker and M.Bailes, p367
Kawai, N., Tamura, K., Shibata, S., 1997, in preparation
Kundt, W., Schaaf, R., 1993, Ap & SpSc, 200, 251
Kurt, V.A., Komberg, B.V., Sokolov, V.V., Zharikov, S.V., Pavlov, G.G., 1997, IAU Cir. 6533
Manning, R., Willmore, P., 1994, MNRAS, 266, 635
Michel, F.C., 1991, *Theory of Neutron Star Magnetospheres*, University of Chicago Press, Chicago, IL
Mignani, R., Caraveo, P.A., Bignami, G.F., 1997a ApJ, 476, 246
Mignani, R., Caraveo, P.A., Bignami, G.F., 1997b, in *Advance in Space Research*, Contribution to the COSPAR Meeting, 1996 July 14-21 Birmingham, eds. P.Caraveo et al., in Press
Ögelman, H., Finley, J.P., 1993, ApJ, 413, L31
Ögelman, H., Finley, J.P., Zimmerman, H.U., 1993, Nat, 361, 136.

Ögelman, H., 1995, in *The Lives of Neutron Stars* eds A. Alpar, U. Kilizóglu & J. van Paradijs, Kluwer Academic Publishers, p.101
Pavlov, G.G., Shibanov, Y.A., Zavlin, V.E., Meyer, R.D., 1995, in *The Lives of Neutron Stars* eds A. Alpar, U. Kilizóglu & J. van Paradijs, Kluwer Academic Publishers, p71
Pavlov, G.G., Stringfellow, G.S., Cordova, F.A., 1996, ApJ, 467, 370
Pacini, F., 1967, Nat, 221, 567
Possenti, A., Mereghetti, S., Colpi, A., 1997 to appear in A&A
Possenti, A., Mereghetti, S., Stella, L., 1996, in *Röntgenstrahlung from the Universe*, eds H.U. Zimmermann, J. Trümper and H. York, p177, MPE-Report 263
Romani, R.W., 1987, ApJ, 313, 718
Safi-Harb, S., Ögelman, H., Finley, J.P., 1995, ApJ, 439, 722
Saito, Y., Kawai, N., Kamae, T., Shibata, S., Dotani, T., Kulkarni, S.R., 1996, ApJ, 477, L37
Seward, F.D., Wang, Z.R., 1988, ApJ, 332, 199
Shearer, A., et al., 1996a, IAU Circ., 6502
Shearer, A., et al. 1996b, preprint
Stark, A.A., Gammie, C.F., Wilson, R.W., Bally, W.J., Linke, R., Heiles, C., Hurwitz, M., 1992, ApJS, 79, 77
Taylor, J.H., Cordes, J.M., 1993, ApJ, 411, 674
Taylor, J.H., Manchester, R.N., Lyne, A.G., Camilo, F., 1995, unpublished
Thompson, D.J., 1996, in *IAU Colloquium 160*, eds S.Johnston, M.A.Walker and M.Bailes, p307
Toor, A., Seward, F.,D., 1977, ApJ, 216, 560
Trümper, J., 1995, Reviews in modern astronomy, 8, 1
Trümper, J., Supper, R., Becker, W., 1997, in preparation
Ulmer, M.P., et al., 1994, ApJ, 417, 738
Umeda, H., Shibazaki, N., Nomoto, K., Tsuruta, S., 1993, ApJ, 408, 186
Verbunt, F., Kuiper, L., Belloni, T., Johnston, H.M., de Bruyn, A.G., Hermsen W. and Van der Klis M., 1996, A&A, 311, L9
Yancopoulos, S., Hamilton, T.T., Helfand, D.J., 1994, ApJ, 429, 832
Zavlin, V.E., Shibanov, Yu., Pavlov, G.G., 1995, Astron. Letters, 21, 149
Zavlin. V.E., Pavlov, G.G., Shibanov, Y.A. and Ventura, J., 1995, A&A, 297, 441
Zavlin, V.E., Pavlov, G.G., 1997, submitted to A&A
Zimmerman, H.U., Becker, W., Belloni,T., Doebereiner, S., Izzo, C., Kahabka, P., Schwentker, O., 1994, MPE-Report 244

This article was processed by the author using Springer-Verlag LaTeX A&A style file *L-AA* version 3.